DOI:
10.1039/c8an02218f

Document Version
Peer reviewed version

Towards identifying the mode of action of drugs using live-cell FTIR spectroscopy

Ali Altharawi, Khondaker Miraz Rahman and K. L. Andrew Chan*

e-mail: ka_lung.chan@kcl.ac.uk

School of Cancer and Pharmaceutical Science, King's College London, SE1 9NH, UK

Abstract

Fourier transform infrared spectroscopy (FTIR) has been shown to be a promising tool for identifying the mode of action of drugs. However, most previous studies have focused on the analysis of fixed or dried cells. The measurement of living cells has the advantage of obtaining time series data and the *in-situ* approach eliminates the need for fixing or drying the cells. In this study, the potential of live-cell FTIR method for the identification of the mode of action of drugs was demonstrated. Four different drugs were tested, with two of the drugs having the same mode of action (tamoxifen and toremifene), and the other two having different modes of action (imatinib and doxorubicin). Live cells were treated in the four drugs at and below the IC50 level (i.e. the concentration of drug required to inhibit the growth of cells by 50%), and the changes to their spectra after the addition of drugs were monitored over a 24-hour period. Principal component analysis (PCA) of the spectral data shows that drugs with different modes of action are well-separated, while the drugs with same mode of action are grouped together. The results also show that at IC50, the separation appears to be the clearest at 2 hours for imatinib, tamoxifen/toremifene and 6 hours for doxorubicin. However, at 50% IC50 drug concentration, the separation appears to be the best at longer incubation time, i.e. 24 hours, for all four drugs. In conclusion, live-cell FTIR has shown to be able to distinguish and group spectral signatures of cells treated with drugs of known modes of action after a relatively short time of exposure. Further collection of live-cell data would enable an algorithm to be developed for the prediction of the modes of action of novel drugs, which can help in the preclinical drug screening process.

Introduction

The drug discovery process involves a high-throughput screening assays which use either *in vitro* cell-free bioassays or an *in-silico* approach, followed by *in vitro* validation. However, cell-free assays and *in silico* approaches lack mechanistic information and cellular penetration considerations, resulting in a high attrition of compounds and high cost. Current biochemical *in vitro* cell assays that are used in anticancer developments rely on destructive techniques that are expensive, time consuming and laborious.[1, 2] Fourier transform infrared (FTIR) spectroscopy is a chemically specific, label-free and non-destructive analytical method for biological samples.[3] The application of FTIR spectroscopy for drug-cells interaction analysis has attracted much attention,[4, 5] with number of studies focusing on dry or fixed cells.[5-10] The method has shown great promises in characterising the mode of action of drugs based on the changes to the chemical composition of the drug-treated cells

at specific time point.[11] However, the development in the FTIR measurement of live cells has allowed measurement of living cells at different time points during treatment.[12-20] Another advantage of this *in situ* approach is that drying or fixing of cells is not carried out, reducing the chance of introducing experimental artefacts. Chemical changes such as cellular metabolites, proteins and nucleic acids inside the living cells can be followed in real time after the addition of drugs, maximising the potential of this technique for the understanding of the mechanism of drugs action.

Measurement of living cells has been a challenging task because cells are generally cultivated in culture medium, i.e. surrounded by water, and the most common medium requires a humid atmosphere with 5% CO_2 supplement for the buffer to maintain a physiological pH. We have shown that plain phosphate-buffered saline solution cannot maintain the viability of cells for more than a few hours, with rapid changes to the cellular composition observed.[21] Effectively, mini-CO_2 incubators were built in the early live cell spectroscopic studies, or a specific flow cell was required to maintain the viability of the cells during measurement.[22] Furthermore, water has strong absorbance in the mid-IR region, which often requires the path length of the IR light in the sample to be controlled and small (<10 µm). Spectral regions where water has strong absorption (~1650-1620 cm^{-1}) often results in a poor signal to noise ratio (SNR) that severely reduces the applicability of this method in the study of living cells. Raman spectroscopy has the advantage of low water absorption and shown interesting applications for the study of cellular changes in the Raman spectra after drug application and intracellular probing of drugs and its metabolites. However, the main drawback of conventional Raman spectroscopy is the longer acquisition time which limits its use in drug screening approach.[23-26]

Infrared synchrotrons with brightness of several orders of magnitude higher than an ordinary Globar source have been used to partially overcome this problem. Using synchrotron sources, the measurement of infrared spectra of living cells within a reasonable time frame has been successfully demonstrated,[27, 28] including the characterisation of normal cells from carcinoma,[29] response of cells to mechanical stress,[30] apoptotic pathways,[31] chemical stress,[12] optical stimulation,[32] protein aggregation,[17, 33] drug actions,[10] toxicity in living algae[34] and imaging with subcellular spatial resolution using ZnS hemispheres.[35] However, access to synchrotron facilities are limited and therefore measurements of living cells that can be carried out in an ordinary laboratory remains highly desirable. The use of bench-top (non-synchrotron) FTIR imaging to measure a population of living cells in transmission mode has shown that the SNR can be improved by using principle component reconstruction, allowing the distinguishing of cells before and after the treatment of drugs.[36, 37] Other recent demonstrations of non-synchrotron based single living cells transmission imaging include the use of a pair of CaF_2 hemispheres to increase magnification and remove spherical and chromatic aberrations in a microfluidic device. A set of spectra of live cells with high SNR were obtained, with spectral changes identified before and after cell attachment.[14]

Apart from transmission FTIR, the study of living cells utilising attenuated total reflection (ATR) sampling methods was shown to be suitable for live cells studies.[38] ATR FTIR imaging has been previously employed to study the dissolution of pharmaceutical substances in order to avoid over-absorbance due to the presence of water.[39] Furthermore, the sampling volume of the ATR method is restricted by the depth of penetration, which is typically ~2 µm above the surface of the ATR element where cells are attached. The infrared absorbance signal is mostly contributed from the attached cell because the depth of penetration of the IR light is typically smaller than the thickness

of an attached cell, which is on the order of 4-5 µm.[40] Several earlier works have demonstrated that the ATR FTIR method is suitable for live cells studies.[22, 41-49] We have demonstrated the use of the CO_2 independent L15 medium to simplify the measurement and shown that drug concentration as little as 15 µM can be detected in live cells.[15, 16]

While most of the live cell-drug interaction studies were focused on the differences before and after the treatment of the drug, there been no direct comparison using live cells measurements of the effect of different drugs with different modes of action. In this preliminary work, we are demonstrating for the first time that live-cell FTIR using the multi-bounce ATR approach combined with principal component analysis (PCA), can be a powerful technique to separate drugs with different modes of action while grouping drugs with the same modes of action. The overall aim is to develop this method as a complementary tool in the drug screening process.

The interest of this study is breast cancer cells and MDA-MB-231 is among breast cancer cells that are used in the National Cancer Institute 60 (NCI60) screening approach.[2, 50] It is an invasive, hard to treat cancer and attract a lot of interest for finding new anticancer drugs. We will use this cell line in the demonstration of live cells study using multi-bounce ATR FTIR approach.

Experimental Section

Multi-bounce ATR-FTIR accessory

A temperature controlled 10-reflection (10 internal reflections on the sample side) ATR accessory trough plate (HATR, Pike technologies) and 45° ZnS ATR element (80 mm X 10 mm X 4 mm, Crystan Ltd., UK) were used. The effective path length obtained in the living cells produced from this accessory is approximately 20-30 µm, with a depth of penetration ($\mathbf{d_p}$) nearly 2-3 µm. The trough plate has a measurement surface of about 500 mm^2, where live cells adhere and continuously measured.

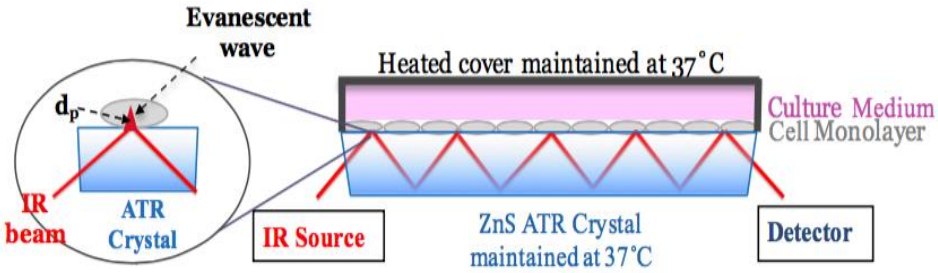

Figure 1: Schematic of the multi-reflection ATR-FTIR measurement setup

Live cell preparation

MDA-MB-231 cells (obtained from the maintained stock (passage number 4) of cell lines from Dr Khondaker Miraz Rahman, Institute of Pharmaceutical Science, King's College London) were maintained in T25 cell culture flasks using DMEM high glucose medium with 10% FBS, 1% MEM NEAA, 2 mM L-glutamine, 100 U/mL penicillin and 100 U/mL streptomycin and incubated in a 5% CO_2 and 37°C incubator. The cells were trypsinised and harvested when they reached ~90%

confluence and then centrifuged into a pellet. The pellet was then re-suspended in L15 medium, supplemented with 10% FBS, 1% MEM NEAA, 2 mM L-glutamine, 100 U/mL penicillin and 100 µg/mL streptomycin, to reach a cell density of ~ 0.5 x 10^6 cells/mL and total of 2.0 mL of suspension (i.e ~ 1.0 X 10^6 cells). The cell suspension was directly seeded onto the multi-bounce trough plate controlled at 37 °C and sealed with a heated glass cover lid at 37 °C, to control the temperature in the measurement chamber. After 24 hours of incubation, the high seeding density ensured that cells are attached to the measurement surface as a monolayer with high (~90%) confluence. A reflective optical microscope with a 10x objective (L2003 microscope fitted with a digital camera) was used to confirm the confluence and attachment of cells to the measurement surface (**see supplementary Figure 1S**).

Determination of cell viability

Cell viability was determined using standard MTT (3-(4,5-dimethylthiazol-2-yl)-2,5-diphenyltetrazolium bromide) tetrazolium reduction assay.[51] In brief, MDA-MB-231 Cells (2 x 10^4 cells/well) were seeded in a 96-well plate and allowed to grow in the L15 medium for 24 hours at 37°C, until a comparable confluence (~90%) to the ATR-FTIR experiment was observed in the wells. The medium was then replaced by the L15 medium, which contains different concentrations of tamoxifen, toremifene, imatinib (dissolved in DMSO) and doxorubicin (dissolved in water) and was then incubated for another 24 hours. In all treatments, the final concentration of DMSO was maintained at 0.1% DMSO. Afterward, the supernatant of each well was removed, washed once with PBS medium and replaced by 100 µL (0.5 mg/mL) of MTT in L15 medium. The 96-well plate was incubated for another 2 hours before the MTT solution was discarded and then 100 µL/well of DMSO was added to dissolve the resulted formazan product. The absorbance was measured at 570 nm, with reference at 630 nm in a Spectra MAX 190 multi-well plate reader. The relative cell viability percentage was calculated by comparing absorbance of treated cells with a control, where 0.1% DMSO in L15 medium was applied instead of tamoxifen solution.

FTIR measurement of samples

A continuous scan FTIR spectrometer (Frontier, Perkin Elmer Ltd., UK), fitted with a room temperature deuterated triglycin sulfate (DTGS) detector, was used to acquire FTIR spectra. After seeding the cells in the ATR trough for 24 hours, the cells on the ATR element were exposed to the IC50 (or 50% of the IC50) value of tamoxifen, toremifene, imatinib and doxorubicin by adding appropriate amounts of 50 mM stock solution (in L15 medium, 0.1% DMSO). The cells exposed to drugs were measured with a scanning time of 11 minutes. A spectrum was measured every 20 minutes, and all measurements were acquired with a spectral resolution of 8 cm^{-1} and a spectral range of 1800 to 900 cm^{-1}. The strong Norton-Beer apodization function and self-phase correction were chosen for the interferogram process. Spectrum 10 software (Perkin Elmer Ltd., UK) was used for all data pre-treatment processing. Spectra of cells were continuously monitored from the moment after seeding the cells on the ATR element for 24 hours. For control, 0.1% DMSO was added to the medium and measured for another 24 hours. A spectrum of L15 medium was used as a background to obtain the full spectra of cells with the water vapour subtracted. For difference spectra, the first spectrum of cells immediately after the addition of drugs was used as a background to highlight the changes in live cells because of introducing the compound. All measurements were made in triplicate.

Principal Component Analysis (PCA)

PCA was carried out using PyChem Software (http://pychem.sourceforge.net/).[52] This analysis was applied to reduce the dimension of the spectroscopic data. Correlation matrix and Nonlinear Iterative Partial Least Squares (NIPALS) were selected for the PCA analysis. Before analysis, spectra were truncated to 2000-900 cm^{-1} wavenumber and then an interactive baseline correction using the Spectrum 10 software (Perkin Elmer) was performed based on the minima absorbance at 2000, 1800, 1757, 1480, 1000 and 950 cm^{-1} wavenumbers. Vector normalisation was calculated in Microsoft ®Excel 10, in which spectra were divided by the square root of the sum of the mean intensities squared. PC1, PC2 and PC3 were selected to represent the spectral variances, as they account for more than 85% of the variances (**see supplementary Figure 2S**) and plotted at different time points.

Results and Discussion

A representative ATR-FTIR spectra of live MDA-MB-231 cells in the first 24 hours after seeding at ~2.0 X 10^5 cell/cm^{-2} acquired by multi-reflection ATR-FTIR spectroscopy in the region 1800-900 cm^{-1} is shown in **Figure 2**. Cells were seeded at a high density to obtain a high coverage of the ATR measuring surface to maximise the signal from the cell. The analysis is focused in the 1800-900 cm^{-1} region because this is the region that contains the most information about the chemical composition of the cell where water does not have strong absorbance, except the amide I region, which is excluded in the PCA analysis. Although measurements were made every 20 min, with a scanning time of 11 min, a shorter measurement time and higher measurement rate can be achieved using a MCT detector but it was found to be not necessary in this work because the changes in the cell were found to be relatively slow.[15] The first hour after seeding cells on the ATR element has shown a relatively weak absorbance of ~0.04 absorbance units for the amide II band at ~1545 cm^{-1} **(Figure 2)**. The amide II band absorbance has rapidly increased in the next 8 hours, followed by a slow but steady increase from the 12 to 24 hours, which indicates the attachment of MDA-MB-231 cells on the ZnS ATR crystal is completed within the first 12 hours, followed by cell growth. Cells were left for 24 hours to allow enough time for intimate adherence on the ATR crystal, which reproducibly reaching the plateau absorbance of ~0.2. The changes in amide II absorbance after 24 hours of seeding is relatively small, and therefore the chance of detecting subtle cellular changes induced by anticancer drugs will be increased, particularly with a high SNR gained by using the current FTIR method.

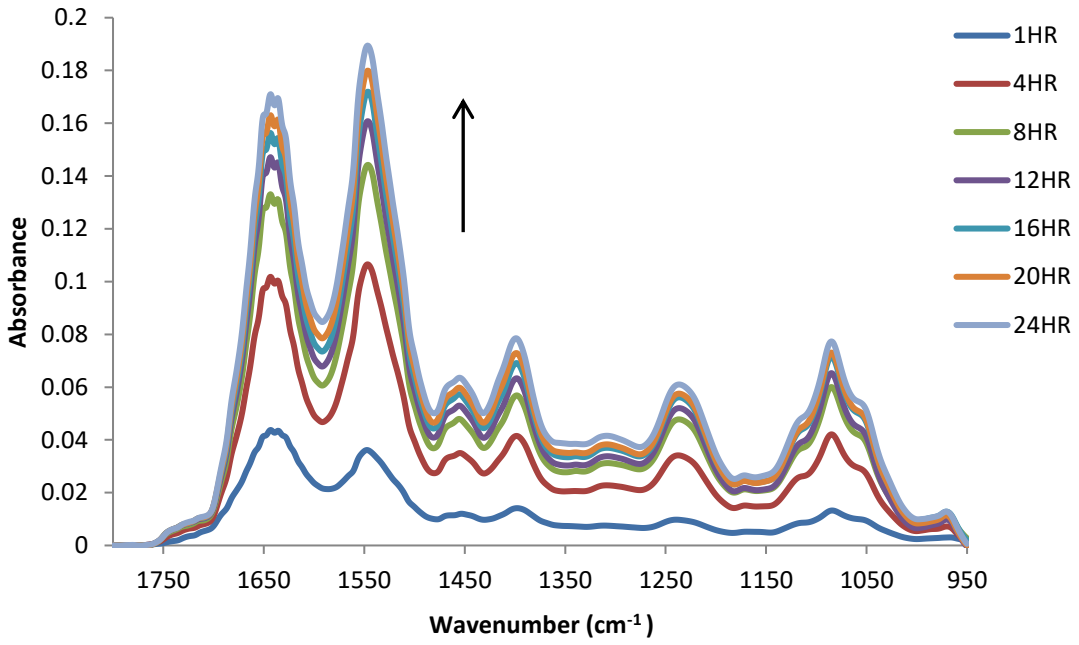

Figure 2: A typical set of ATR-FTIR spectra of live MDA-MB-231 cells for 24 hrs after seeding (Control). A straight line between 1800-950 cm^{-1} was used to baseline the spectra.

In this study, four drugs (tamoxifen, toremifene, imatinib and doxorubicin) were tested at their IC50s (***the concentration of drug required to inhibit the growth of cells by 50%)*** determined by standard MTT assay[51] instead of using the same concentration for each drug. The IC50 is a commonly used concentration to normalise and study the effects of anticancer compounds. This will help in normalising the differences between drug performance due to the difference in the rate of drug uptake and transport. Previous studies have shown that these drugs exhibit their cytotoxic effect against MDA-MB-231 cells through targeting different cellular pathways that are essential for survival and proliferation of cells. For example, imatinib has been shown to have anti-proliferative, cytostatic and apoptotic effect due to its ability to block the platelet derived growth factor receptor (PDGF-Rβ).[53-57] Additionally, tamoxifen has been shown to induce apoptosis mediated by an oestrogen-independent pathway in triple negative breast cancer cell lines (MDA-MB-231, MDA-MB-468, MDA-MB-453 and SK-BR-3).[58, 59] Doxorubicin is a DNA alkylator which is used in the treatment of triple negative breast cancer and its activity against MDA MB 231 is well documented.[60, 61] **Figure 3A** shows an example of the MTT assay result for the MDA-MB-231 cells treated with (1-100 µM) of tamoxifen for 24 hours is shown and the IC50 was found to be at ~25 µM (refer to **Table 1**). When exposing the attached live MDA-MB-231 cells on the ATR element to this concentration, where a 50% decrease in cell is expected, Figure 3B shows an approximately 37% decrease in amide II absorbance relative to the control. The difference could be a result of the relatively high confluence of cells used in the live cell ATR test, as compared to the MTT assay, and the fact that the amide II absorbance in the live cell FTIR measurement reflects on cell detachment upon cell death, while the MTT assay is based on the reduction in mitochondria activities. Nevertheless, the cytotoxic effect of the drug is clearly shown by both measurement methods.

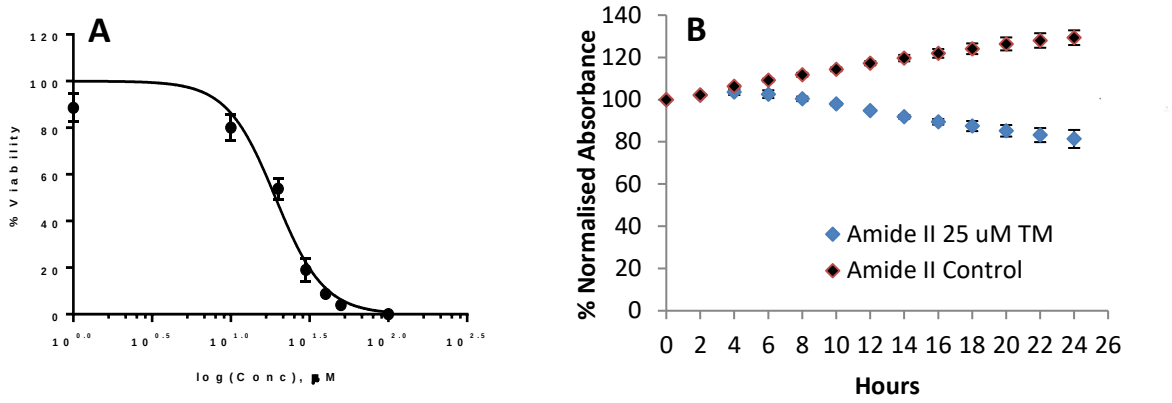

Figure 3: A) Cell Viability Percentage of MDA-MB-231 treated with tamoxifen for 24 hrs. B) Amide II (~1546 cm^{-1}) normalised absorbance (percentage) of live MDA-MB-231 cells as a function of time following the addition of 0.1% drug vehicle (DMSO; Black) and 25 µM Tamoxifen (Blue) for 24 hrs. Peaks normalised at absorbance value when 0.1% DMSO and 25 µM Tamoxifen added to cells (time 0 = 100 %)

It is important to emphasise that the FTIR measurements were repeated three times by seeding cells from separate tissue culture flasks for each condition. The small standard deviation (shown by the error bars) in **Figure 3B** clearly shows the high reproducibility of the current FTIR method in measuring the response of live cells after exposure to the drug vehicle and IC50 concentration of anticancer drugs. Difference spectra (using the first spectrum measured immediately after adding drugs as a background) was used to show the subtle spectral changes of cells after the exposure to anticancer drugs. To maintain the clarity of presentation, vector normalised spectra collected at the 2^{nd}, 4^{th} and 6^{th} hours of treatment have been selectively presented, which reflect the changes in the cellular components as a function of time after drug exposure and are shown in **Figure 4**.

Table 1: Summary of Drugs' Mode of Action

Drug	Mode of Action	IC50 (µM)
Tamoxifen	1. Selective Oestrogen Receptor Modulator (SERMs) also known as Oestrogen-Dependent Pathway mainly in ER-positive breast cancer (e.g. MCF7) 2. Oestrogen-Independent Pathway in triple negative breast cancer cell (e.g. MDA-MB-231)	~25.0
Toremifene	1. Selective Oestrogen Receptor Modulator (SERMs) also known as Oestrogen-Dependent Pathway mainly in ER-positive breast cancer (e.g. MCF7) 2. Oestrogen-Independent Pathway in triple negative breast cancer cell (e.g. MDA-MB-231)	~30.0
Imatinib	Tyrosine Kinase Inhibitor (TKI)	~50.0
Doxorubicin	DNA-Intercalating Agent	~ 3.0

From the visual inspection of the spectra, it is evidence that the anticancer drugs of different modes of action induced significant spectral changes at different time points that are different from each other and from control, while drugs with the same mode of action show similar changes. For instance, the difference spectra of control cells in **Figure 4** at different time points resemble the typical spectrum of cell as shown in **Figure 2**. In comparison to the control cells, cells exposed to doxorubicin have shown a decrease in the absorbance in the 1085 cm^{-1} and 1050 cm^{-1} regions with a clearer drop after 4 and 6 hours of exposure while amide II bands ~ 1545 cm^{-1} was relatively similar **(Figure 4B and 4C)**. These changes were previously observed with PC3 cells treated with 1.0 µM doxorubicin and might be associated with DNA phosphates backbone changes because of the DNA disintegrating effect of doxorubicin (a well-known intercalating agent).[16] The exposure of cells to imatinib highlighted a significant increase in the absorbance peaks at 1600 cm^{-1} and 1400 cm^{-1}, which coincide with the symmetrical and asymmetrical stretching modes of carboxylate peaks, suggesting an increase in carboxylate metabolites in the cells as shown in **Figure 4 A-C**. The cells treated with tamoxifen and toremifene have also shown an increase in the 1600 cm^{-1} and 1400 cm^{-1} peaks but at a lower level, comparing to imatinib, in the 2 hours and 4 hours treatment. However, the spectral change for tamoxifen, toremifene and imatinib become similar in the 1600-1400 cm^{-1} region after 6 hours of exposure. Although these spectral changes were similar in the 1600-1400 cm^{-1} region, it can be observed that imatinib induced these changes faster than tamoxifen and toremifene (**Figure 4A**). It is important to emphasise that a remarkable similarity between tamoxifen and toremifene in the 1600-950 cm^{-1} region in all hours of treatments were clearly shown in **Figure 4** demonstrating that anticancer drugs with same mode of actions are likely to cause similar cellular changes. The peaks observed (i.e. 1600 cm^{-1} and 1400 cm^{-1}) were not detected in the ATR-FTIR spectra of imatinib, tamoxifen and toremifene (see supplementary **Figure 6S**), which mainly associated with the cellular spectral changes in response to drugs.

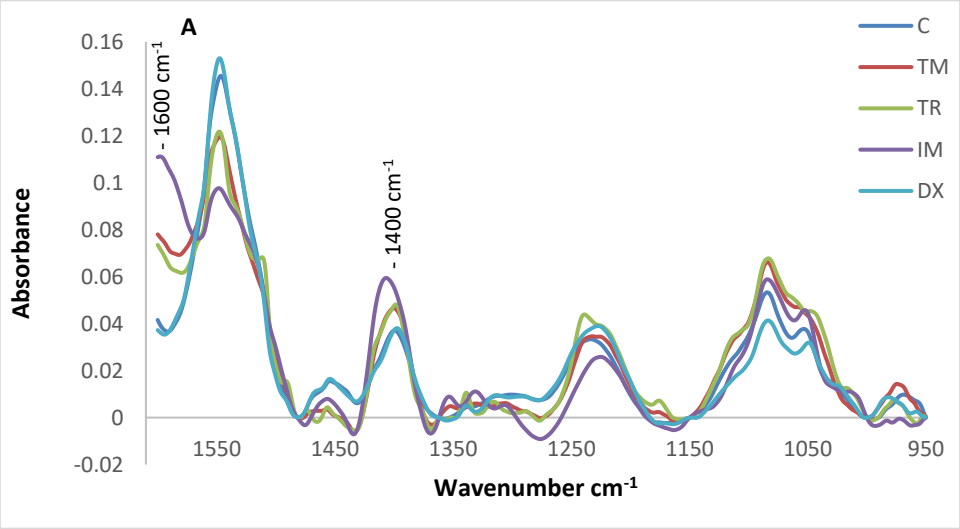

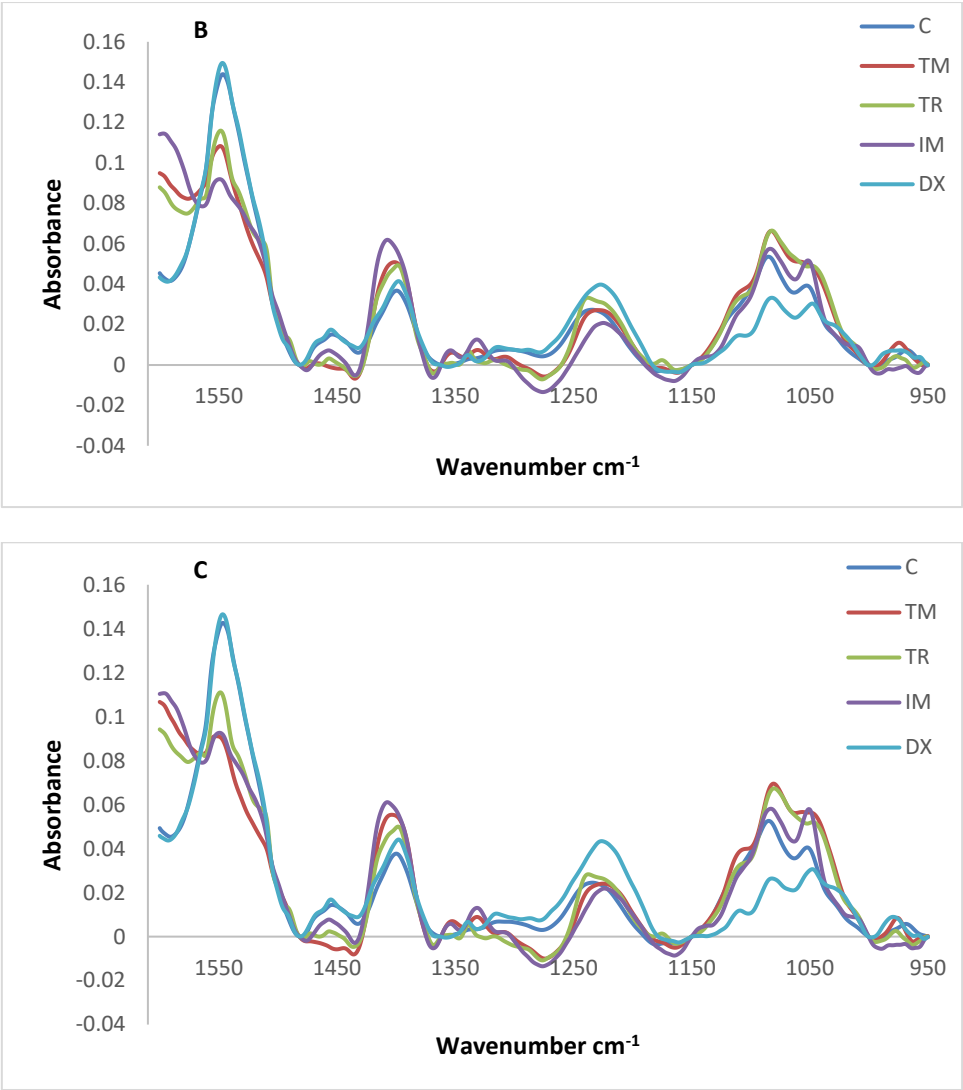

Figure 4: FTIR vector normalised difference spectra of live MDA-MB-231 cells after exposure to 0.1% DMSO (drug vehicle; control(C)) and IC50 of tamoxifen (TM), toremifene (TR), imatinib (IM) and doxorubicin (DX) for 2, 4 and 6 hours (A, B, C, respectively). The spectra presented are average of three repeated measurements (see supplementary Figure 3S the spectra with error bars).

PCA was also used for the analysis of the subtle cellular changes of cells exposed to tamoxifen, toremifene, imatinib and doxorubicin at IC50. The mode of actions of drugs used in this study are summarised in **Table 1**. The PCA of cellular response of control and cells exposed to IC50 of tamoxifen, toremifene, imatinib and doxorubicin in the 2nd hour, 4th hour and the 6th hour were shown in **Figure 5 A-C,** respectively. Further analysis using 2nd derivative vector normalised difference spectra of the same data is shown in (supplementary **Figure 4S and 5S**). First, it can be observed that the repeated experiments of untreated control cells are tightly clustered together in the score plot, demonstrating the reproducibility of this method (**Figure 5 A-C, blue circle**). In **Figure 5A**, PC1 (68.28% of variances) of the 2nd hour exposure to drugs highlighted changes in the 1600 and 1400 cm^{-1} absorbance peaks which confirms the observation made in (**Figure 4A**). In addition, this PC, which gives a clear separation of cells treated with tamoxifen, toremifene and imatinib from

control and doxorubicin, highlights changes in the 1240-950 cm^{-1} where absorbance peaks of asymmetric PO_2^- of nucleic acids, lipids and phosphorylated proteins (~1237 cm^{-1}), C−O of protein side chain groups and carbohydrate (~1150 cm^{-1}), symmetric PO_2^- of nucleic acids and PO_4^{-2} phosphorylated proteins, C−O−C and C−O−P of polysaccharides (~1080 cm^{-1}), C−O of carbohydrates (~1050-1036 cm^{-1}) and PO_4^{-2} of phosphorylated proteins and nucleic acids (~990-970 cm^{-1}). PC2 represents 15.15% of variances and mainly separates tamoxifen and toremifene from control, imatinib and doxorubicin and shows absorbance peaks at 1510 cm^{-1}, 1243 cm^{-1}, 1174 cm^{-1}, and 1022 cm^{-1}. To consider the origin of these peaks, ATR-FTIR spectra of 10 mM of drugs in 10% DMSO (see supplementary Figure 6S) were collected to compare with this PC loading, which has shown that the peaks at 1510 cm^{-1}, 1243 cm^{-1} and 1174 cm^{-1} are originated from tamoxifen and toremifene accumulation in cells in the first 2 hours of treatment. In addition to these peaks, PC2 also highlighted changes in the 1150-950 cm^{-1} associated with changes in carbohydrates and phosphorylated cellular compounds as previously described and none of these peaks are originated from drug spectra (see supplementary **Figure 6S**). PC3 (**Figure 5B**) accounts for 7.25% of the variances provides little separation between the different treatment. The PCA of the 4th hour exposure to drugs is shown in (**Figure 5C and 5D**). PC1 (74.81 % of variances) highlighted changes in the 1600 and 1400 cm^{-1} absorbance peaks and changes in the 1150-950 cm^{-1}. In a similar pattern, it separated cells treated with tamoxifen, toremifene and imatinib from control and doxorubicin. However, the separation between tamoxifen or toremifene and imatinib has reduced compared to the PC1 of the 2nd hour data. In addition, PC2 of the 4th hour (represents 12.19% of variances) separated doxorubicin treated cells from control cells as shown in (**Figure 5C,** red square) and highlighted the spectral changes in the carbohydrates and phosphates region at 1150-970cm^{-1}. Most importantly, absorbance peaks of tamoxifen and toremifene become less significant in this PC2 and contributed minimally to the separation between tamoxifen, toremifene and imatinib. Comparing to the spectrum of doxorubicin shown in Figure 6S to the loading plot of PC2, no similarity can be observed highlighting that the separation of control from doxorubicin treated cells are mainly based on the changes in the cellular composition rather than drug accumulation. PC3 (**Figure 5D**) accounts for 5.16% of the variances mainly separates doxorubicin from control. **Figure 5E and 5F** show the PCA of the 6th hour exposure in which PC1 accounts for 72.60% of variances and separates cells treated with tamoxifen, toremifene and imatinib from control and doxorubicin treated cell, similar to that of the PC1 from the 4th hour data (**Figure 5C**). However, there was no clear separation between tamoxifen or toremifene and imatinib in PC1 from the 6th hour data. PC2 (14.55%) and PC3 (5.98%) separate doxorubicin treated cells from control and clearly demonstrates the changes in the 1240-970 cm^{-1} associated with changes in the phosphorylated proteins, nucleic acids and carbohydrates. Comparing to the drug spectra in Figure 6S, the PCA has shown that spectral changes are not due to the accumulation of drug in both the 4th and 6th hour data. In all cellular changes described here, PC loadings show several changes in the region of 1240-970 cm^{-1} which mainly associated with carbohydrates and phosphorylation/dephosphorylation of proteins and nucleic acids. Imatinib is a tyrosine kinase inhibitor (**TKIs**) and exert its action by inhibiting the phosphorylation process of proteins. These changes have been previously shown in PC12 cells during neuronal differentiation induced by NGF and were mainly assigned with protein phosphorylation.[62] Tamoxifen and toremifene are selective oestrogen receptor modulators (SERMs) and characterised by their competition with oestrogen for binding to the oestrogen receptor (ER) and ultimately inhibiting the proliferation of ER-positive breast cancer tissue or so-called ER-dependent pathway. Additionally, tamoxifen has been shown to have an ER-independent effects in triple negative breast

cancer cells (e.g. MDA-MB-231) associated with inhibition of cancerous inhibitor of protein phosphatase 2A (CIP2A) and phospho-Akt (p-Akt).[59] The similarity between the effect of imatinib, tamoxifen and toremifene from the 6th hour onward could be attributed to their influence on the phosphorylation/dephosphorylation status of proteins, carbohydrates and nucleic acids. However, at this stage, it is not possible to confirm the specific biomolecules that caused these changes due to the overlapping of cellular component peaks in this region. It is important to emphasise that doxorubicin also showed cellular changes in the phosphates and carbohydrates region mainly in the 1150-970 cm^{-1}, but the PC loadings in the 2nd, 4th and 6th hr clearly showed no overlapping in separation between doxorubicin treated cells and tamoxifen, toremifene and imatinib cells. This suggests that doxorubicin has a different mode of action on the MDA-MB-231 cells in comparison to tamoxifen, toremifene and imatinib. Although the early hours (i.e. 2nd hr) showed some overlap between doxorubicin and control (**see Figure 5A**), the separation becomes very clear in the longer exposure time (**see Figure 5C-F**) and indicates the time-dependent effect on the cells.

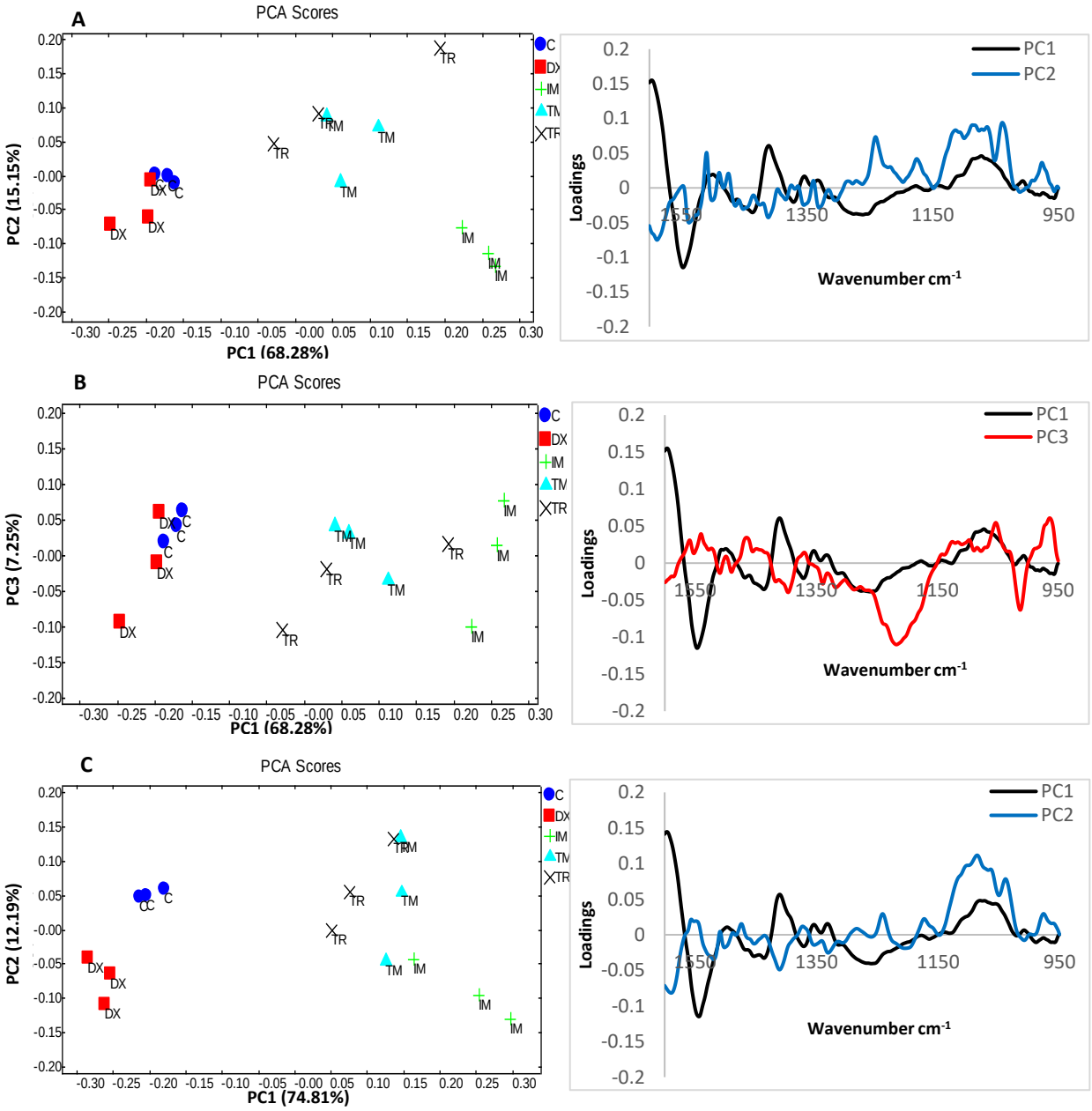

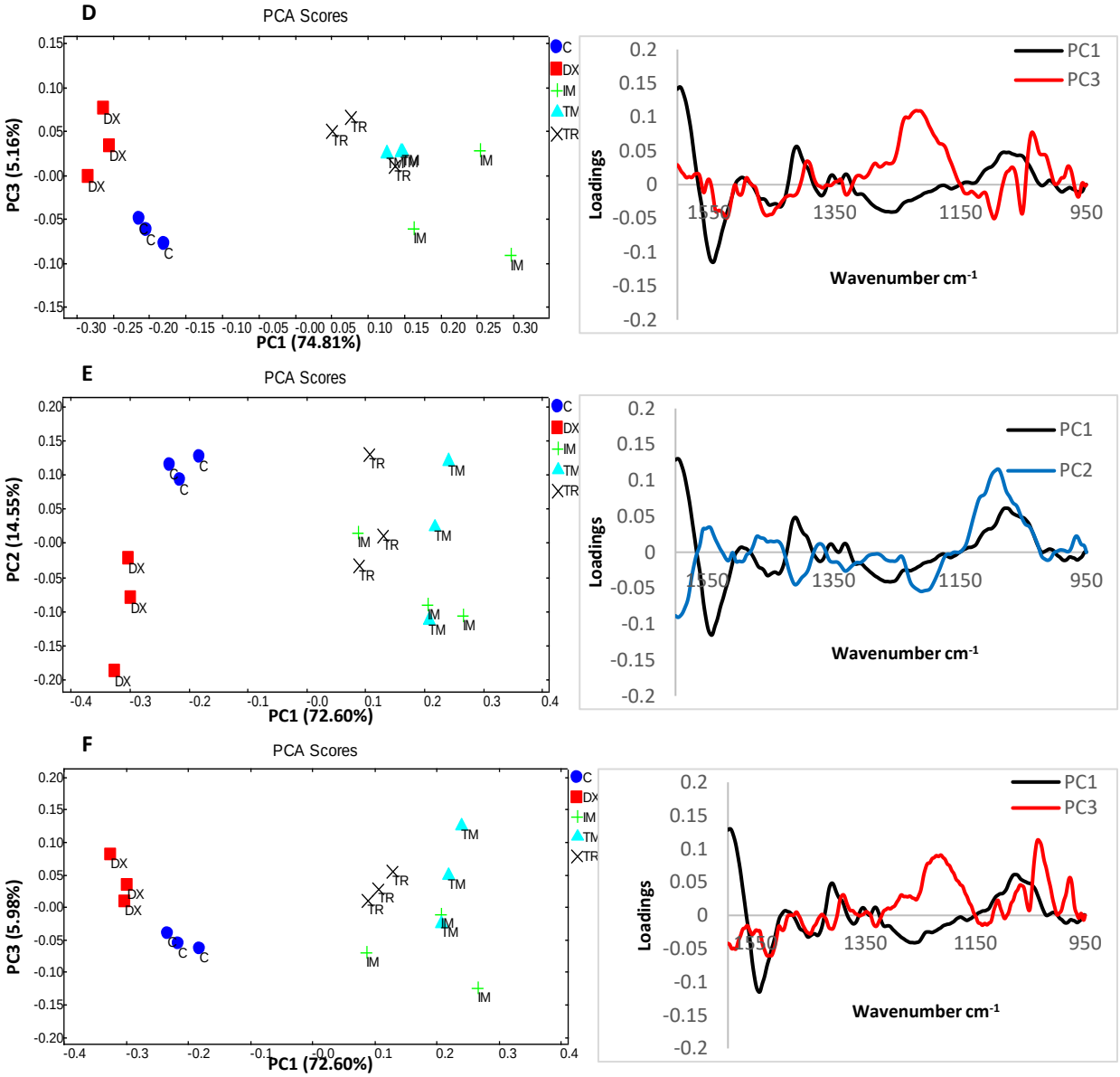

Figure 5: PCA scores and their corresponding loadings of FTIR vector normalised difference spectra of live MDA-MB-231 cells after exposure to 0.1% DMSO (Control) and IC50 of tamoxifen (TM), toremifene (TR), imatinib (IM) and doxorubicin (DX) in the 2nd hr (A and B), 4th hr (C and D) and 6th hr (E and F).

We further investigated the sensitivity of live cell ATR FTIR method in the detection of cellular responses at lower concentrations (e.g. 50% of IC50 value). Previous study on non-cytotoxic dose using Raman imaging has shown that it is clinically important to measure the effect of drug to cells at low concentrations.[63] To our knowledge, it is the first time that the ATR method was used to examine live cells response to sub-IC50 concentrations. PCA was applied to detect spectral changes in cells in response to the 50% of IC50 concentration of tamoxifen, toremifene, doxorubicin and imatinib (~12.5, 15, 1.0 and 25 µM, respectively). With the lower drug concentration, the results have shown that the separation between drug treated cells happens at longer incubation time. The PC1 (78.23% of variances, **Figure 6A**) of the 6th hour of exposure to 50% IC50 has separated the response of cells exposed to imatinib from control, tamoxifen, toremifene and doxorubicin. However, cells treated with tamoxifen, toremifene and doxorubicin were not separated. This may be

due to the dose-dependent response of cells to these drugs or the resistant mechanism against these drugs employed by the cells at lower concentration, as cells show only limited response to anticancer drugs in the early hours. On the other hand, PC2 (13.95% variances, **Figure 6A**) separated the control cells from the drug treated cells and shows that the differences are mainly in the carbohydrates and phosphate band regions. In the PC3 (4.12% variances, **Figure 6B**), two peaks of tamoxifen and toremifene at 1243 cm^{-1} and 1174 cm^{-1}were detected (see supplementary **Figure 6B**) due to the accumulation of drugs in the cells. Despite these peaks, PC3 also show changes in the region 1150-970 cm^{-1} associated with carbohydrates and phosphates that is not originated from the drugs themselves. Further investigation of a longer exposure of cells in drug (i.e. at 24 hours) is shown in (**Figure 6C and 6D**). In contrast to the early response, PC1 (60.01 % of variances) and PC2 scores (27.3% of variances) and its corresponding loading plots gives a clear separation to all drugs and the PC loadings did not show any contribution from the drugs spectra. This demonstrated that the separation in the PCA is based on the cellular response rather than drug accumulation.

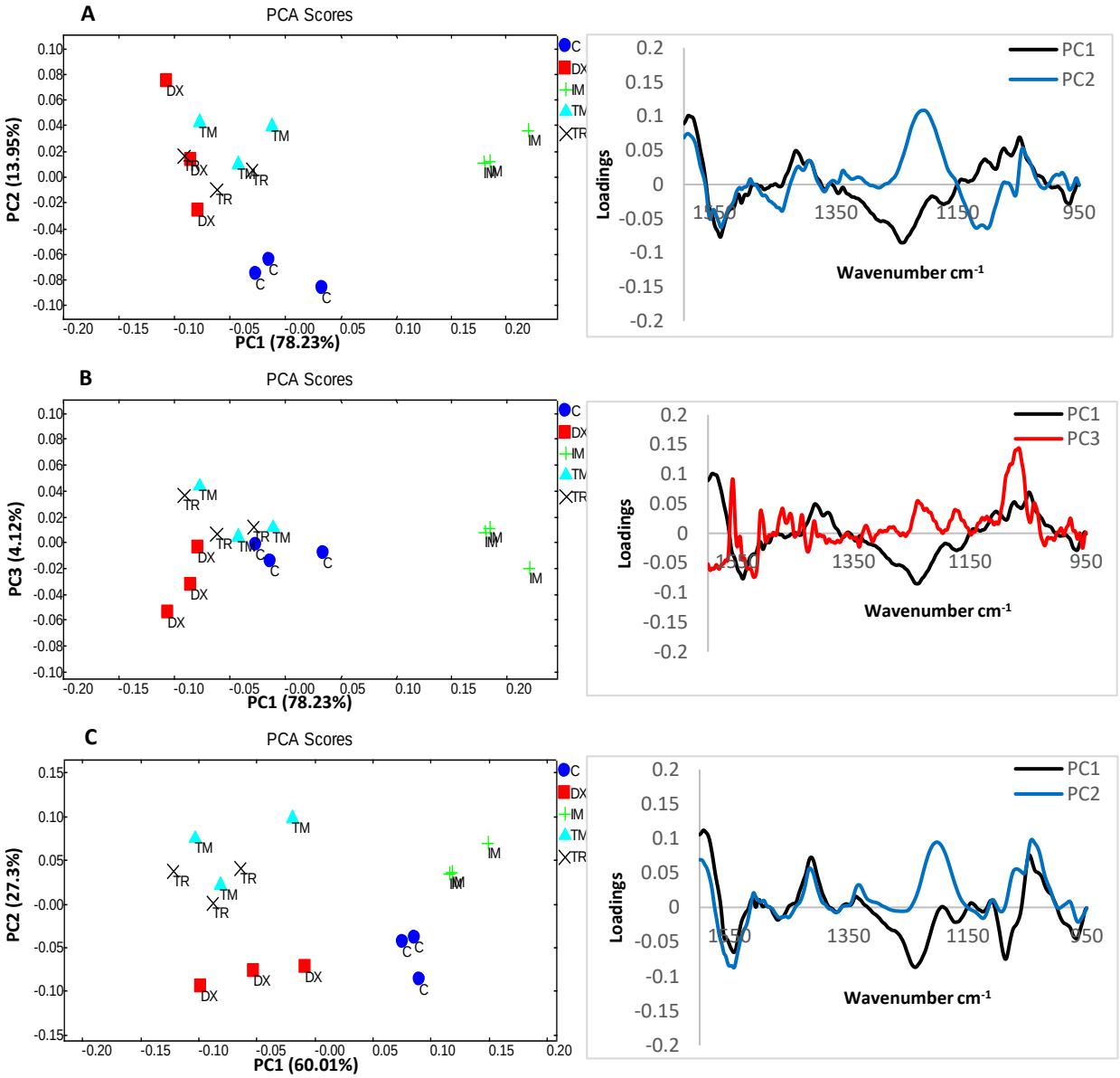

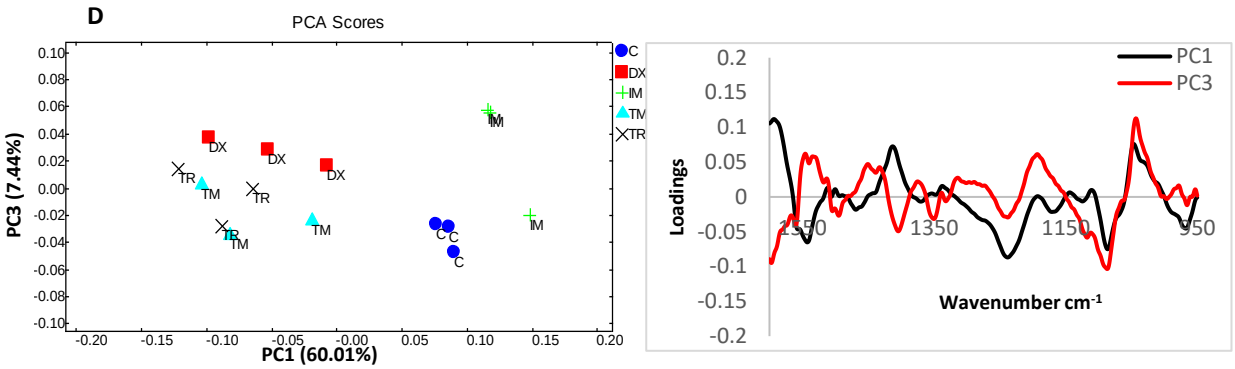

Figure 6: PCA scores and their corresponding loadings of FTIR vector normalised difference spectra of live MDA-MB-231 cells after exposure to 0.1% DMSO (Control) and 50% IC50 of tamoxifen (TM), toremifene (TR), imatinib (IM) and doxorubicin (DX) in the 6th hr (A and B) and 24th hr (C and D).

To obtain an overall view of the spectral changes that give the best separation between drugs and control, pairwise PCA analysis of control versus each of the drugs in the 24th hour of cells treated with 50% IC50 were performed as it has been shown to provide the best separation (**Figure 6C**). In all pairwise PCA analysis, PC1 provides a clear separation between the control and the treated cells (**Figure 7A-C**) and accounts for more than 78% of the variances. The PC1 loadings (**Figure 7D**) demonstrate that most spectral changes are observed in the 1240-970 cm^{-1} region, which is sensitive to the changes in the phosphate moiety particularly for tamoxifen, toremifene and imatinib.[64] While these spectral changes occur in the same IR region, it is clearly shown that the cellular components that lead to such pattern of absorbance are remarkably different. In fact, this is expected as these drugs are known to target different cellular pathways as previously described. For instance, tamoxifen has been shown to induce apoptosis because of its phosphatases activity that lead to the downregulation of p-Akt pathway. This can produce a change to the absorbance in the $\nu_{sym}(PO_2)^-$ and $\nu_{asym}(PO_2)^-$ vibrational mode due to the inhibition of protein phosphorylation. In addition, PC1 loadings of control versus doxorubicin in **Figure 7D (Red line)** shows a clear spectral change in three IR absorbance bands at 1225, 1085, 970 cm^{-1} that are associated with DNA phosphates backbone. Imatinib inhibits the tyrosine kinases activity and expected to cause different changes in the phosphates absorbance due to the reduction in the phosphorylation of the tyrosine side chain (**Figure 7D, Blue line**).”

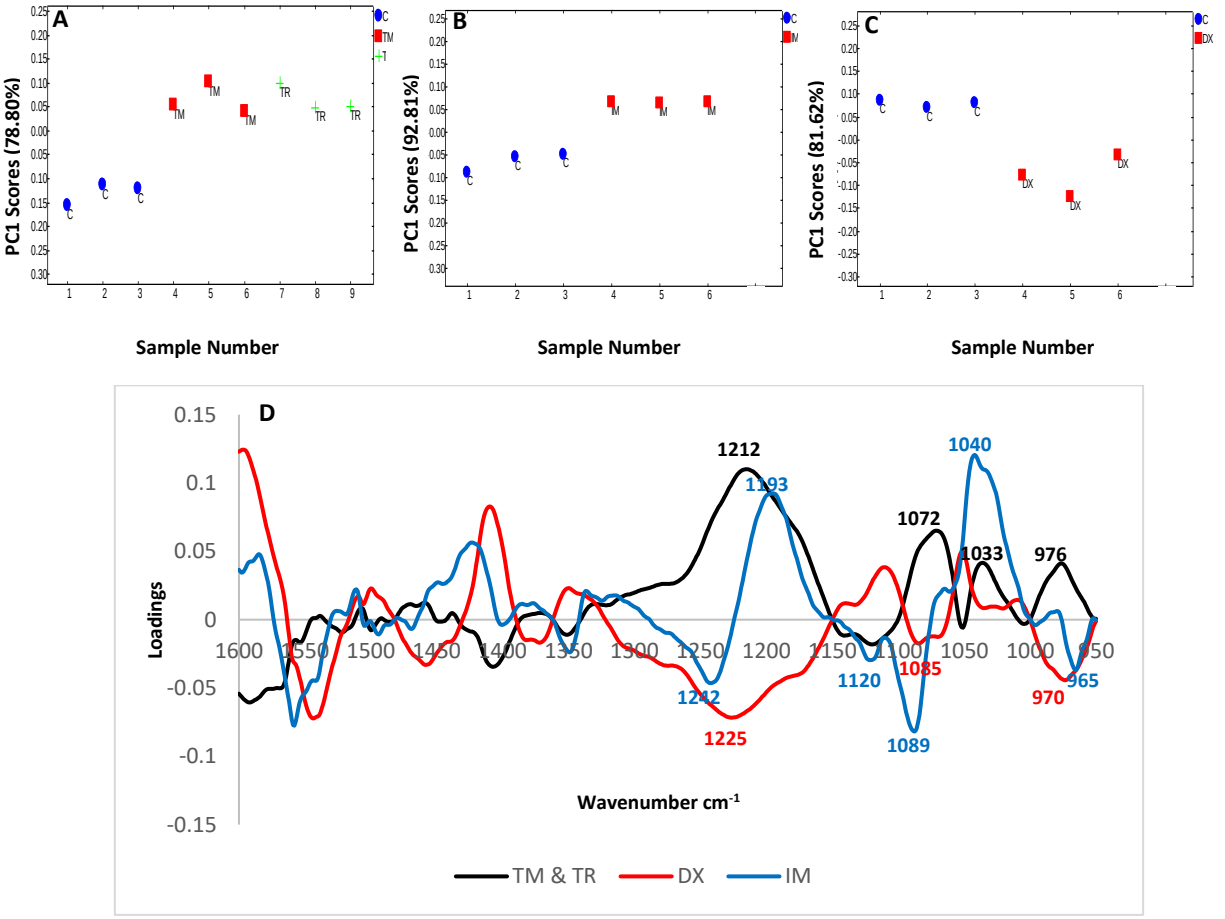

Figure 7: (A) shows the pairwise PC1 scores of control (1-3) versus tamoxifen (4-6) and toremifene (7-9). (B) shows control (1-3) versus imatinib (4-6) and (C) shows control (1-3) versus doxorubicin (4-6). (D) represents the corresponding PC1 loadings of tamoxifen and toremifene (black), imatinib (blue) and doxorubicin (red). All samples were run in triplicates.

Conclusions

The combined live-cell FTIR spectroscopy with principal component analysis has shown to be able to distinguish the different responses from the testing cell (MDA-MB-231) treated with four different drugs of known modes of action. Drugs that have the same mode of action (tamoxifen and toremifene) were grouped together, while drugs with different modes of action (imatinib and doxorubicin) were differentiated in the analysis. Using PCA, clear separation between drugs with different modes of action was found, with a short drug treatment time of less than 6 hours at IC50 concentration. When cells were treated with lower drug concentrations (i.e. 50% of IC50), clear separation was found at a later treatment stage of 24 hours. The results demonstrated the potential of using this complementary tool for pre-clinical drug screening studies, which could improve the efficiency of drug screening programs by confirming the modes of action of drugs without recourse to expensive and laborious biochemical assays. The time course study has revealed that the best separations are obtained at between 2-6 hours of drug treatment at IC50, with the best separation of drug found at different time points depending on mode of action of the drug. The pairwise PCA analysis has further reinforce the relationship between spectral changes to the known mode of

action of drugs. This highlights the advantages of the demonstrated technique where many time points can be measured in a single measurement. The next step is to combine the live cell FTIR method with high-throughput technique such as FTIR imaging to study multiple drug samples in individual wells in parallel.[65]

Acknowledgement

Ali Atharawi thanks Prince Sattam Bin Abdulaziz University (Saudi Arabia) for his PhD sponsorship.

Reference

1. A. M. Burger and H. Fiebig, in *Handbook of Anticancer Pharmacokinetics and Pharmacodynamics*, Springer, 2014, pp. 23-38.
2. M. Suggitt and M. Bibby, *Clinical Cancer Research*, 2005, **11**, 971-981.
3. M. J. Baker, J. Trevisan, P. Bassan, R. Bhargava, H. J. Butler, K. M. Dorling, P. R. Fielden, S. W. Fogarty, N. J. Fullwood, K. A. Heys, C. Hughes, P. Lasch, P. L. Martin-Hirsch, B. Obinaju, G. D. Sockalingum, J. Sule-Suso, R. J. Strong, M. J. Walsh, B. R. Wood, P. Gardner and F. L. Martin, *Nature Protocols*, 2014, **9**, 1771-1791.
4. A. Mignolet, A. Derenne, M. Smolina, B. R. Wood and E. Goormaghtigh, *Biochimica et biophysica acta*, 2016, **1864**, 85-101.
5. L. E. Jamieson and H. J. Byrne, *Vibrational Spectroscopy*, 2017, **91**, 16-30.
6. F. Draux, P. Jeannesson, C. Gobinet, J. Sule-Suso, J. Pijanka, C. Sandt, P. Dumas, M. Manfait and G. D. Sockalingum, *Ana Bioanal Chem.*, 2009, **395**, 2293-2301.
7. G. Bellisola, M. Della Peruta, M. Vezzalini, E. Moratti, L. Vaccari, G. Birarda, M. Piccinini, G. Cinque and C. Sorio, *Analyst*, 2010, **135**, 3077-3086.
8. K. R. Flower, I. Khalifa, P. Bassan, D. Demoulin, E. Jackson, N. P. Lockyer, A. T. McGown, P. Miles, L. Vaccari and P. Gardner, *Analyst*, 2011, **136**, 498-507.
9. A. Derenne, M. Verdonck and E. Goormaghtigh, *Analyst*, 2012, **137**, 3255-3264.
10. J. L. Denbigh, D. Perez-Guaita, R. R. Vernooij, M. J. Tobin, K. R. Bambery, Y. Xu, A. D. Southam, F. L. Khanim, M. T. Drayson, N. P. Lockyer, R. Goodacre and B. R. Wood, *Scientific Reports*, 2017, **7**.
11. C. Hughes, G. Clemens and M. J. Baker, *Trends in Biotechnology*, 2015, **33**, 429-430.
12. K. L. Munro, K. R. Bambery, E. A. Carter, L. Puskar, M. J. Tobin, B. R. Wood and C. T. Dillon, *Vibrational Spectroscopy*, 2010, **53**, 39-44.
13. M. J. Tobin, L. Puskar, R. L. Barber, E. C. Harvey, P. Heraud, B. R. Wood, K. R. Bambery, C. T. Dillon and K. L. Munroe, *Vibrational Spectroscopy*, 2010, **53**, 34-38.
14. K. L. Chan and S. G. Kazarian, *Analyst*, 2013, **138**, 4040-4047.
15. P. L. Fale and K. L. Chan, *Analytical Chemistry*, 2014, **86**, 11673-11679.
16. P. L. Fale, A. Altharawi and K. L. Chan, *Biochimica et Biophysica Acta (BBA)-Molecular Cell Research*, 2015, **1853**, 2640-2648.
17. P. Gelfand, J. S. Randy, E. Stavitski, D. R. Borchelt and L. M. Miller, *Analytical Chemistry*, 2015, **87**, 6025-6031.
18. E. Mitri, S. Kenig, G. Coceano, D. E. Bedolla, M. Tormen, G. Grenci and L. Vaccari, *Analytical Chemistry*, 2015, **87**, 3670-3677.
19. K. L. Chan and S. G. Kazarian, *Chemical Society Reviews*, 2016, **45**, 1850-1864.
20. J. Doherty, G. Cinque and P. Gardner, *Applied Spectroscopy Reviews*, 2017, **52**, 560-587.
21. M. K. Kuimova, K. L. Chan and S. G. Kazarian, *Applied Spectroscopy*, 2009, **63**, 164-171.
22. K. I. Miyamoto, P. Yamada, R. T. Yamaguchi, T. Muto, A. Hirano, Y. Kimura, M. Niwano and H. Isoda, *Cytotechnology*, 2007, **55**, 143-149.
23. K. Ock, W. Jeon, E. O. Ganbold, M. Kim, J. Park, J. H. Seo, K. Cho, S. W. Joo and S. Y. Lee, *Analytical chemistry*, 2012, **84**, 2172-2178.

24. S. F. El-Mashtoly, D. Petersen, H. K. Yosef, A. Mosig, A. Reinacher-Schick, C. Kötting and K. Gerwert, *Analyst*, 2014, **139**, 1155-1161.
25. Z. Farhane, F. Bonnier, A. Casey and H. Byrne, *Analyst*, 2015, **140**, 4212-4223.
26. R. Smith, K. L. Wright and L. Ashton, *Analyst*, 2016, **141**, 3590-3600.
27. D. A. Moss, M. Keese and R. Pepperkok, *Vibrational Spectroscopy*, 2005, **38**, 185-191.
28. H. Y. Holman, H. A. Bechtel, Z. Hao and M. C. Martin, *Analytical Chemistry*, 2010, **82**, 8757-8765.
29. R. Zhao, L. Quaroni and A. G. Casson, *Analyst*, 2010, **135**, 53-61.
30. G. Birarda, G. Grenci, L. Businaro, B. Marmiroli, S. Pacor, F. Piccirilli and L. Vaccari, *Vibrational Spectroscopy*, 2010, **53**, 6-11.
31. G. Birarda, D. E. Bedolla, E. Mitri, S. Pacor, G. Grenci and L. Vaccari, *Analyst*, 2014, **139**, 3097-3106.
32. L. Quaroni, T. Zlateva and E. Normand, *Analytical chemistry*, 2011, **83**, 7371-7380.
33. L. M. Miller, M. W. Bourassa and R. J. Smith, *Biochimica et biophysica acta-Biomembranes*, 2013, **1828**, 2339-2346.
34. X. Y. Xin, G. H. Huang, X. Liu, C. J. An, Y. Yao, H. Weger, P. Zhang and X. J. Chen, *Environmental Pollution*, 2017, **226**, 12-20.
35. K. L. Chan, P. L. Fale, A. Altharawi, K. Wehbe and G. Cinque, *Ana Bioanal Chem.*, 2018, **410**, 6477-6487.
36. E. J. Marcsisin, C. M. Uttero, M. Miljkovic and M. Diem, *Analyst*, 2010, **135**, 3227-3232.
37. E. J. Marcsisin, C. M. Uttero, A. I. Mazur, M. Miljkovic, B. Bird and M. Diem, *Analyst*, 2012, **137**, 2958-2964.
38. N. J. Harrick, *Internal reflection spectroscopy*, Harrick Scientific Corporation, New York, Third edn., 1987.
39. S. G. Kazarian and K. L. Chan, *Macromolecules*, 2003, **36**, 9866-9872.
40. C. L. Curl, C. J. Bellair, T. Harris, B. E. Allman, P. J. Harris, A. G. Stewart, A. Roberts, K. A. Nugent and L. M. Delbridge, *Cytometry Part A*, 2005, **65A**, 88-92.
41. T. B. Hutson, M. L. Mitchell, J. T. Keller, D. J. Long and M. J. W. Chang, *Analytical Biochemistry*, 1988, **174**, 415-422.
42. M. Schmidt, T. Wolfram, M. Rumpler, C. P. Tripp and M. Grunze, *Biointerphases*, 2007, **2**, 1-5.
43. R. T. Yamaguchi, A. Hirano-Iwata, Y. Kimura, M. Niwano, K. I. Miyamoto, H. Isoda and H. Miyazaki, *Applied Physics Letters*, 2007, **91**.
44. M. K. Alam, J. A. Timlin, L. E. Martin, D. Williams, C. R. Lyons, K. Garrison and B. Hjelle, *Vibrational Spectroscopy*, 2004, **34**, 3-11.
45. J. A. Timlin, L. E. Martin, C. R. Lyons, B. Hjelle and M. K. Alam, *Vibrational Spectroscopy*, 2009, **50**, 78-85.
46. R. Yamaguchi, A. Hirano-Iwata, Y. Kimura, M. Niwano, K. Miyamoto, H. Isoda and H. Miyazaki, *Journal of Applied Physics*, 2009, **105**.
47. W. Y. Yang, X. L. Xiao, J. Tan and Q. Y. Cai, *Vibrational Spectroscopy*, 2009, **49**, 64-67.
48. Y. Aonuma, Y. Kondo, A. Hirano-Iwata, A. Nishikawa, Y. Shinohara, H. Iwata, Y. Kimura and M. Niwano, *Sensors and Actuators B-Chemical*, 2013, **176**, 1176-1182.
49. P. L. Fale and K. L. Chan, *Vibrational Spectroscopy*, 2017, **91**, 59-67.
50. S. L. Holbeck, J. M. Collins and J. H. Doroshow, *Molecular cancer therapeutics*, 2010, **9**, 1451-1460.
51. T. Mosmann, *Journal of immunological methods*, 1983, **65**, 55-63.
52. R. M. Jarvis, D. Broadhurst, H. E. Johnson, N. O'Boyle and R. Goodacre, *Bioinformatics*, 2006, **22**, 2565-2566.
53. C. Mundhenke, M. Weigel, S. R. Schmidt, I. Meinhold-Heerlein, C. Schem, D. O. Bauerschlag, W. Jonat and N. Maass, *Journal of Clinical Oncology* 2005, **23**, 3210-3210.

54. C. J. Malavaki, A. E. Roussidis, C. Gialeli, D. Kletsas, T. Tsegenidis, A. D. Theocharis, G. N. Tzanakakis and N. K. Karamanos, *The FEBS journal*, 2013, **280**, 2477-2489.
55. N. Pilco-Ferreto and G. M. Calaf, *International journal of oncology*, 2016, **49**, 753-762.
56. A. Kadivar, M. Ibrahim Noordin, A. Aditya, B. Kamalidehghan, E. T. Davoudi, R. Sedghi and H. Akbari Javar, *International journal of molecular medicine*, 2018, **42**, 414-424.
57. S. Modi, A. D. Seidman, M. Dickler, M. Moasser, G. D'Andrea, M. E. Moynahan, J. Menell, K. S. Panageas, L. K. Tan and L. Norton, *Breast cancer research and treatment*, 2005, **90**, 157-163.
58. S. Mandlekar and A. N. Kong, *Apoptosis*, 2001, **6**, 469-477.
59. C. Y. Liu, M. H. Hung, D. S. Wang, P. Y. Chu, J. C. Su, T. H. Teng, C. T. Huang, T. T. Chao, C. Y. Wang, C. W. Shiau, L. M. Tseng and K. F. Chen, *Breast Cancer Research*, 2014, **16**, 431-439.
60. C. J. Lovitt, T. B. Shelper and V. M. Avery, *BMC cancer*, 2018, **18**, 41.
61. H. A. Wahba and H. A. El-Hadaad, *Cancer biology medicine*, 2015, **12**, 106-116.
62. L. Chen, H. Y. Holman, Z. Hao, H. A. Bechtel, M. C. Martin, C. Wu and S. Chu, *Analytical Chemistry*, 2012, **84**, 4118-4125.
63. F. Draux, C. Gobinet, J. Sulé-Suso, M. Manfait, P. Jeannesson and G. D. Sockalingum, *Analyst*, 2011, **136**, 2718-2725.
64. F. Syberg, Y. Suveyzdis, C. Kötting, K. Gerwert and E. Hofmann, *Journal of Biological Chemistry*, 2012, **287**, 23923-23931.
65. K. L. Chan and S. G. Kazarian, *Lab Chip.*, 2006, **6**, 864-870.